JOURNAL OF COMPUTATIONAL PHYSICS 111, 62–73 (1994)

Accurate One-Dimensional Computation of Frontal Phenomena by PLIM

MARKKU RAJAMÄKI AND MIKA SAARINEN

Nuclear Engineering Laboratory, Technical Research Centre of Finland, P.O. Box 208, 02151 Espoo, Finland

Received March 22, 1993; revised August 12, 1993

We introduce a new method for solving systems of one-dimensional hyperbolic partial differential equations and present the first applications of this method. The piecewise linear interpolation method PLIM is shown to have the capability to preserve the shape of a propagating distribution and great applicability. Various difficult flow problems, such as the strong convection problem, the convection diffusion problem, and the reaction–diffusion problem, have been solved. In addition, the approximate hyperbolic equations technique (AHET) to handle the diffusion terms is introduced.

1. INTRODUCTION

A primary problem in computational fluid dynamics has been in the avoidance of the typical numerical errors in solutions to hyperbolic partial differential equations. These errors, often called numerical diffusion and numerical dispersion, cause erroneous damping and oscillations in the most essential part of the solution. The numerical solutions by standard discretization methods converge to the rigorous solution very slowly when the mesh size is decreased, and, e.g., the finite element method (FEM) suitable to many numerical problems does not yield essential gains over more elementary methods.

We introduce a new shape-preserving characteristics method, piecewise linear interpolation method, PLIM [1], for solving one-dimensional hyperbolic equations and show the results of its first applications.

The goal of the development work of PLIM was to create a numerical scheme which is applicable and accurate always when conventional methods are accurate and which is able to treat propagating piecewise linear distributions accurately on a mesh grid. In the one-dimensional time-dependent case, interpolation with the piecewise linear polynomial approximation containing two unknown parameters yields the desired shape preserving scheme. The conservation laws are not violated either. The discretization mesh needed and the numerical performance of the solution procedure are in direct proportion to the physical complexity.

A numerical method should be applicable to solve problems as generally as possible. In this paper we show that PLIM is capable of solving general problems using within itself conventional local linearization of the functions including unknown variables.

Although simple solutions can be achieved accurately, it is difficult to ensure that there are no other numerical difficulties when more challenging problems are solved. Hence we have applied PLIM to solve various flow problems. It has been applied very successfully to the transport of a scalar quantity, adiabatic gas flow in a pipe, stratified two-phase flow, dynamics of the slip between phases in two-phase flow, gas dynamics, and various convection–diffusion problems and, more generally, to problems with derivatives of second order.

PLIM solutions makes it possible to achieve a converged solution with a very simple procedure by solving PLIM equations in both directions on the computational mesh. This is advantageous when parallel computing is used. The convergence of the method has been illustrated by numerical examples.

The basic idea of PLIM is to represent the unknown variables at each boundary of the mesh cell in terms of a piecewise linear approximation. Other kinds of shape-preserving methods which use information within the mesh cell are described, for example, in [10–12].

Since PLIM is capable of preserving the shape of a propagating distribution, physical diffusion is not more suppressed by numerical errors, and it is very essential to govern diffusion in the framework of PLIM. Convection–diffusion is generally considered to be a very challenging problem, particularly with strong convection.

A particular technique utilizing PLIM has been developed for equations containing diffusion terms. The technique allows the diffusion process to propagate together with a propagating front. It is shown that with these

0021-9991/94 $6.00

equations, quite complicated convection–diffusion and reaction–diffusion problems can be solved successfully.

2. BASIS OF THE PIECEWISE LINEAR INTERPOLATION METHOD

PLIM and the corresponding computer code are applied to one-dimensional partial differential equations of the first order,

$$\frac{\partial}{\partial t}\mathbf{U}+\frac{\partial}{\partial z}\mathbf{F}=\mathbf{P}, \tag{1}$$

where

$$\mathbf{U}=\mathbf{U}(\mathbf{u}, z, t)$$
$$\mathbf{F}=\mathbf{F}(\mathbf{u}, z, t)$$
$$\mathbf{P}=\mathbf{P}(\mathbf{u}, z, t)$$

and $\mathbf{u}$ is the unknown variable vector, whose dimension is equal to the number of equations.

The equations are programmed into the code in the following form. The different flow problems presuppose only different function-type-like subroutines for $\mathbf{U}$, $\mathbf{F}$, and $\mathbf{P}$. If the equation system is not originally in conservation form, $\mathbf{P}$ includes numerical approximations of the terms that cannot be represented by $\mathbf{U}$ and $\mathbf{F}$.

The z-t space is assumed to be divided into rectangular mesh cells as shown in Fig. 1. In these cells the Jacobian matrices

$$\mathbf{W}_U=\partial\mathbf{U}/\partial\mathbf{u}$$
$$\mathbf{W}_F=\partial\mathbf{F}/\partial\mathbf{u} \tag{2}$$

are evaluated by numerical differences. In the present version of the computer code they are assumed to be constant in each mesh cell. In addition $\mathbf{W}_U$ must not be singular, i.e., $\mathbf{W}_U^{-1}$ must exist.

In the mesh cell, PLIM approximates

$$\mathbf{U}=\mathbf{U}_L+\mathbf{W}_U(\mathbf{u}-\mathbf{u}_L(z, t)) \tag{3}$$

$$\mathbf{F}=\mathbf{F}_L+\mathbf{W}_F(\mathbf{u}-\mathbf{u}_L(z, t)) \tag{4}$$

where the subscript L refers to linear z-t dependent vector functions and forms the cellwise constant velocity matrix

$$\mathbf{V}=\mathbf{W}_F\mathbf{W}_U^{-1}. \tag{5}$$

It follows that $\mathbf{U}$ satisfies the equation

$$\frac{\partial}{\partial t}\mathbf{U}+\mathbf{V}\frac{\partial}{\partial z}\mathbf{U}=\mathbf{P}_M, \tag{6}$$

where $\mathbf{P}_M=\mathbf{P}-(\partial/\partial z)(\mathbf{F}_L-\mathbf{V}\mathbf{U}_L)$.

To form equations that are suitable for the application of the piecewise linear interpolation method the matrix $\mathbf{V}$ is diagonalized

$$\mathbf{V}=\mathbf{S}\mathbf{v}\mathbf{S}^{-1} \tag{7}$$

where $\mathbf{v}$ is a diagonal matrix, which includes eigenvalues of matrix $\mathbf{V}$, i.e., the characteristic velocities of the equation system. The Eq. (1) is an initial value problem in respect of time, thus if the problem is well-posed, all the eigenvalues have to be real. Multiplying Eq. (6) by $\mathbf{S}^{-1}$ yields

$$\frac{\partial}{\partial t}\mathbf{x}+\mathbf{v}\frac{\partial}{\partial z}\mathbf{x}=\mathbf{p}, \tag{8}$$

where $\mathbf{x}=\mathbf{S}^{-1}\mathbf{U}$, $\mathbf{p}=\mathbf{S}^{-1}\mathbf{p}_M$. Hence, N linear uncoupled equations in the mesh cell have been derived. Now $\mathbf{x}$ may be solved using piecewise linear interpolation. The original vector functions $\mathbf{U}$ and $\mathbf{F}$ relate approximately to $\mathbf{x}$ in Eq. (8) as

$$\mathbf{U}=\mathbf{S}\mathbf{x}$$
$$\mathbf{F}=\mathbf{S}\mathbf{v}(\mathbf{x}-\mathbf{S}^{-1}\mathbf{U}_L)+\mathbf{F}_L \tag{9}$$

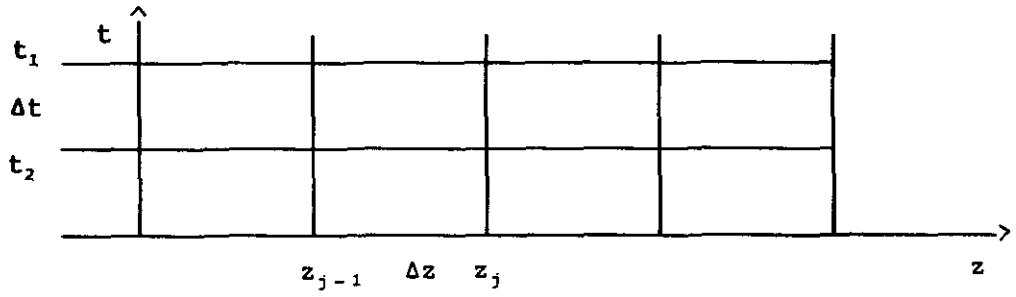

FIG. 1. Discretization mesh.

and as well as that in Eq. (8) **U** and **F** have to satisfy continuity conditions at the boundaries of the mesh cell.

Equation (8) forms a set of independent scalar equations which can be solved separately. Concerning each transport being described by them, the direction of **v** defines the incoming and outgoing boundaries in the mesh cell. The solution to each scalar equation according to the characteristic method is

$$x = x_\theta + \int_\tau p \, d\tau', \tag{10}$$

where x_θ is the interpolated value of x at the incoming boundary of the mesh cell and the integral term is taken along the propagating path.

The major problems in the solution are related to x_θ. If there is no information on the distribution of the variable x in the mesh cell, an accurate numerical solution can be achieved only in the very special case of $\mathbf{v}\,\Delta t/\Delta z = \mathbf{I}$.

The interpolation scheme has the following properties:

— It is such that any distribution at the boundary of the mesh cell can be reasonably approximated.

— It preserves the shape of the propagating distribution in some sense.

— Conservation of x in the mesh cell can be satisfied.

— Overshoots and uncontrolled strong variations can be avoided.

— The propagation of a front within a mesh cell is described, because fronts are very common in flow problems.

— It uses values of only one mesh interval, because then no extra schemes are needed for the end points or for the discontinuity points of the z-interval.

The basic idea of PLIM is to form the distribution of x within the mesh cell by representing the unknown variables at each boundary of the mesh cell in terms of a piecewise linear approximation. Obviously this makes it possible to obtain the propagating ramp solution rigorously.

Define in the interpolated interval

$$x(\theta) = x_L + \Delta x(\theta), \qquad \theta \in [0, 1], \tag{11}$$

where x_L means linear dependence between the endpoints and $\Delta x(\theta)$ is the deviation from x_L. Defining the zeroth and first central moment for piecewise linear function $\Delta x(\theta)$, which has values Δx_j at the points θ_j, one obtains

$$\begin{aligned} m_0 &= \int_0^1 \Delta x(\theta)\, d\theta = \tfrac{1}{2} \sum_j (\theta_{j+1} - \theta_{j-1})\, \Delta x_j \\ m_c &= \int_0^1 (\theta - \tfrac{1}{2})\, \Delta x(\theta)\, d\theta \\ &= \tfrac{1}{6} \sum_j (\theta_{j+1} - \theta_{j-1})(\theta_{j+1} + \theta_j + \theta_{j-1})\, \Delta x_j - \tfrac{1}{2} m_0. \end{aligned} \tag{12}$$

These moments are extremely good parameters, since they relate directly to the conservation and shape of $\Delta x(\theta)$.

Consider the construction of $\Delta x(\theta)$ in a normalized case as shown in Fig. 2; at the endpoints $x(0) = x_1 = 0$ and $x(1) = x_2 = 1$. The conditions to limit the overshoots, undershoots, and the uncontrolled variations of x are

$$\begin{aligned} &0 \leqslant x(\theta) \leqslant 1 \\ &\left| \frac{dx(\theta)}{d\theta} \right| \leqslant \frac{1}{\delta}, \end{aligned} \tag{13}$$

where δ is a numeric parameter. In the general case it is defined as

$$\delta = \delta_1 / |x_2 - x_1| + \delta_2. \tag{14}$$

Values $\delta_1 = 10^{-7}$ and $\delta_2 = 0.05$ have been used in all the following numerical examples.

Under these conditions two piecewise linear approximating function families can be constructed: the triangular approximations and the front-type approximations. These typical approximating functions are shown in Fig. 2 [1]. Variables Δx_h and θ_h in the triangular approximation or θ_{h1} and θ_{h2} in the front-type approximation can be found using Eqs. (12), and hence any values $\Delta x(\theta)$ may be evaluated.

The triangular approximation with the top at positions θ_h and heights Δx_h results in

$$\Delta x(\theta) = \begin{cases} \dfrac{\theta}{\theta_h}\, \Delta x_h, & \text{when} \quad \theta \leqslant \theta_h \\ \dfrac{1-\theta}{1-\theta_h}\, \Delta x_h, & \text{when} \quad \theta_h \leqslant \theta \end{cases} \tag{15}$$

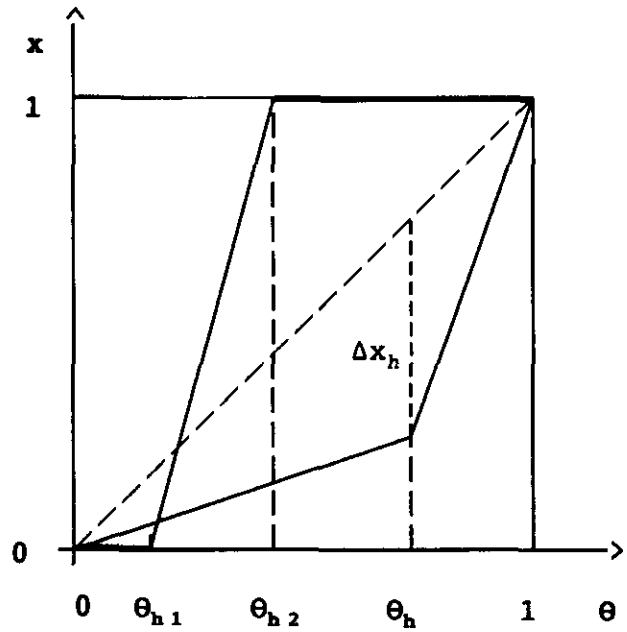

FIG. 2. Normalized piecewise linear approximations.

and the front-type approximation leads to

$$x(\theta)=\begin{cases}0, & \text{when} \quad \theta \leqslant \theta_{h1} \\ \text{linear}, & \text{when} \quad \theta_{h1} \leqslant \theta \leqslant \theta_{h2} \\ 1, & \text{when} \quad \theta_{h2} \leqslant \theta.\end{cases} \tag{16}$$

The next task is to determine the parameters θ_h, Δx_h or θ_{h1}, θ_{h2} as functions of m_0 and m_c. The conditions defined in Eq. (13) restrict the acceptable values of these moments. Hence $\Delta x(\theta)$ must be determined using the values

$$\begin{gathered}|m_0| \leqslant \frac{1}{2}(1-\delta) \\ -\left(2|m_0|-\frac{4}{1-\delta} m_0^2\right) \leqslant m_m \leqslant \left(\frac{1}{2}-|m_0|\right)^2-\frac{1}{4}\delta^2,\end{gathered} \tag{17}$$

where $m_m = 6m_c + 4m_0^2 - |m_0|$.

The new parameter m_m replacing m_c is very useful, because it works as a pattern-recognizing parameter for different piecewise linear approximations, namely,

$$\begin{aligned} &m_m \leqslant 0, \quad \text{triangular approximation} \\ &m_m > 0, \quad \text{front-type approximation.}\end{aligned} \tag{18}$$

Direct application of Eqs. (12), when $m_m \leqslant 0$, yields equations for Δx_h and θ_h in the triangular approximation

$$\begin{aligned} \Delta x_h &= 2m_0 \\ \theta_h &= \frac{3m_c}{m_0}+\frac{1}{2}\end{aligned} \tag{19}$$

and, when $m_m > 0$, for the front-type approximation,

$$\theta_{h1},\ \theta_{h2} = \tfrac{1}{2} - m_0 \pm [(\tfrac{1}{2}-|m_0|)^2 - m_m]^{1/2}. \tag{20}$$

Equations (11)–(20) show how the piecewise linear distribution of $x(\theta)$ can be represented at all boundaries of the mesh cell. The complete representation for one mesh cell is composed of four x_j-values at the corner points and four m_{0j}-values and four m_{cj}-values at the boundaries as shown in Fig. 3. In the mesh cell calculations the values at the incoming boundaries can be considered as known.

Now the unknown value x_4, Fig. 3, can be obtained by direct application of Eqs. (10), (11), (15), (16) and, since $\Delta x(\theta)$ is available, the moments $m_0(\theta_i)$ and $m_c(\theta_i)$ for the partial interval $[\theta_i, 1]$ can be formed and transferred, after some scaling, to the known values of the outgoing boundary.

Two moment values must still be calculated. Since all the

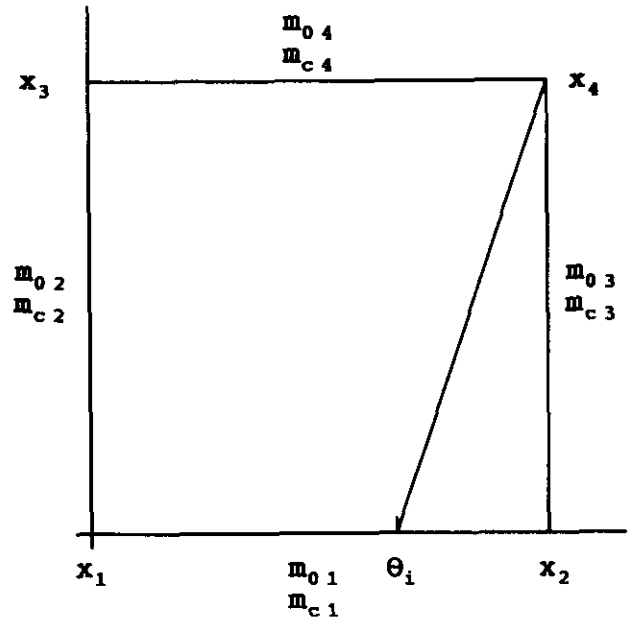

FIG. 3. Variables in the mesh cell.

x_j are now known, moments can be obtained from the equation

$$\frac{\partial}{\partial t}\Delta x + v\frac{\partial}{\partial z}\Delta x = p_m, \tag{21}$$

where

$$p_m = \frac{\partial}{\partial t}x_L + v\frac{\partial}{\partial z}x_L + p.$$

Define

$$\begin{aligned} \theta_{ct} &= \frac{t-t_0}{\Delta t}+\frac{1}{2} \\ \theta_{cz} &= \frac{z-z_0}{\Delta z}+\frac{1}{2} \\ k &= v\frac{\Delta t}{\Delta z} \\ p_m &= p_0 + p_t\theta_{ct} + p_z\theta_{cz}.\end{aligned} \tag{22}$$

Denote the moments along the t-axis and along the z-axis by subscripts t and z, respectively and the z-moments at the former time t_0 by the supercript 0, and the t-moments in flow direction by the subscripts 1 and 2. Integrating Eq. (21) over the mesh cell produces an equatin for m_{0z} and m_{0t},

$$m_{0z} - m_{0z}^0 + k(m_{0t2} - m_{0t1}) = \Delta t\, p_0. \tag{23}$$

An equation for m_{ct} or m_{cz} can be formed by multiplying Eq. (21) by $\theta_{cz} - k\theta_{ct}$ and integrating over the mesh cell:

$$\begin{aligned} m_{cz} - m^0_{cz} - k^2(m_{ct2} - m_{ct1}) \\ - k(m_{0z} + m^0_{0z} - m_{0t2} - m_{0t1})/2 \\ = (p_z - kp_t)\,\Delta t/12. \end{aligned} \tag{24}$$

Five unknown variables per mesh cell can be solved by the preceding procedure, viz. x, m_{0t}, m_{ct}, m_{0z}, m_{cz}. The values m_{0z} and m_{cz} are needed only when the procedure is applied at the next time-step. The moments m_{04} and m_{c4} in Fig. 3 are equal to either m_{0t} and m_{ct} or m_{0z} and m_{cz}, depending on the interpolation case.

The solution of the variable x has now been defined in one mesh cell. When the velocity matrices $\mathbf{V}$ are different in neighbouring mesh cells the values of x and the moments m_0 and m_c cannot be directly transferred to the other mesh cell. The continuity conditions have to be based on the original functions $\mathbf{U}$ and $\mathbf{F}$ in Eq. (1). The conservation property determines that $\mathbf{U}$ has to be treated as temporally continuous and $\mathbf{F}$ as spatially continuous.

At the new time suitable continuity conditions are

$$\begin{aligned} \mathbf{U}^- &= \mathbf{U}^+ \qquad \text{at} \quad z = z_j, \quad t = t_1 \\ \mathbf{F}^- &= \mathbf{F}^+ \qquad \text{at} \quad z = z_j, \quad t = t_1 \\ \int_{\Delta t} (\mathbf{U}^- - \mathbf{U}_L)\,dt &= \int_{\Delta t} (\mathbf{U}^+ - \mathbf{U}_L)\,dt \\ \int_{\Delta z} \theta_{cz}\,(\mathbf{U}^- - \mathbf{U}_L)\,dz &= \int_{\Delta z} \theta_{cz}\,(\mathbf{U}^+ - \mathbf{U}_L)\,dz, \end{aligned} \tag{25}$$

where superscripts $-$ and $+$ refer to the values before and after a time t_1. These conditions are always used at the new time to evaluate $\mathbf{U}^0$, $\mathbf{F}^0$, m^0_{0z}, and m^0_{cz}.

The conditions for the spatial continuity are

$$\begin{aligned} \mathbf{U}_- &= \mathbf{U}_+ \qquad \text{at} \quad z = z_j, \quad t = t_1 \\ \mathbf{F}_- &= \mathbf{F}_+ \qquad \text{at} \quad z = z_j, \quad t = t_1 \\ \int_{\Delta t} (\mathbf{F}_- - \mathbf{F}_L)\,dt &= \int_{\Delta t} (\mathbf{F}_+ - \mathbf{F}_L)\,dt \\ \int_{\Delta t} \theta_{ct}(\mathbf{F}_- - \mathbf{F}_L)\,dt &= \int_{\Delta t} \theta_{ct}(\mathbf{F}_+ - \mathbf{F}_L)\,dt, \end{aligned} \tag{26}$$

where subscripts $-$ and $+$ refer to the values before and after the mesh point z_j. To satisfy these four conditions a new vector $\mathbf{y}$,

$$\mathbf{y} = \mathbf{v}(\mathbf{x} - \mathbf{S}^{-1}\mathbf{U}_L) + \mathbf{S}^{-1}\mathbf{F}_L, \tag{27}$$

and the corresponding moments $\mathbf{m}_{0yt}$ and $\mathbf{m}_{cyt}$ have to be defined. Hence the four conditions in Eq. (26) couple the variables $\mathbf{x}$, $\mathbf{y}$, $\mathbf{m}_{0yt}$ and $\mathbf{m}_{cyt}$ in the z-direction and form the system of equations, which solutions can be utilized in determination of the new values at the incoming boundary of the mesh cell.

The following procedure was used to satisfy the boundary conditions at the boundaries of the mesh cell. The variable is known by the side into which it propagates. Define a vector $\boldsymbol{\theta}_d$, which has the value $\boldsymbol{\theta}_d = 1$, when at the boundary the characteristic velocity points in the direction of the z-axis and $\boldsymbol{\theta}_d = 0$ otherwise. Then it is possible to define deviations $\Delta\mathbf{x}_b$, $\Delta\mathbf{y}_b$, $\Delta\mathbf{m}_{0b}$, $\Delta\mathbf{m}_{cb}$ at the boundaries, for example for $\mathbf{x}$, as

$$\begin{aligned} \mathbf{x}_- &= \mathbf{x}_b + (\mathbf{I} - \theta_d)\,\Delta\mathbf{x}_b \\ \mathbf{x}_+ &= \mathbf{x}_b - \boldsymbol{\theta}_d\,\Delta\mathbf{x}_b \end{aligned} \tag{28}$$

where $\mathbf{x}_b$ refers to values which are propagated to the boundary. Now the $\Delta\mathbf{x}_b$ can be solved;

$$\Delta\mathbf{x}_b = \mathbf{T}\mathbf{x}_b, \tag{29}$$

where $\mathbf{T} = (\mathbf{S}_-(\mathbf{I} - \boldsymbol{\theta}_d) + \mathbf{S}_+\boldsymbol{\theta}_d)^{-1}(\mathbf{S}_+ - \mathbf{S}_-)$.

Now the complete procedure for solving hyperbolic partial differential equations of first order using piecewise linear interpolation method has been presented.

In the general case, when there are characteristic velocities in both directions and the Courant condition ($k < 1$) is satisfied at least in one direction, one cycle of successive mesh cell computations in both directions is needed for the solution. In the more general case, when characteristic velocities are in different directions and the Courant condition is not satisfied in either direction, two to three iterations in both directions are needed. Further, to improve accuracy iterative evaluations of the vector functions, $\mathbf{U}$, $\mathbf{F}$, and $\mathbf{P}$, as well as Jacobian matrices $\mathbf{W}_U$ and $\mathbf{W}_F$, are required.

When complicatedly coupled equations of N variables are solved numerically a computational time per mesh cell must be with any method $\sim N^3$. Generally this is much more than the needed additional effort in the PLIM procedure to solve N scalar equations.

3. THE APPROXIMATE HYPERBOLIC EQUATIONS TECHNIQUE (AHET) TO HANDLE PROBLEMS WITH DERIVATIVES OF SECOND ORDER

It is usual in different kinds of flow problems that a diffusion or viscosity term is involved, and one must also be able to handle derivatives of second order. In strongly convective cases, it is not sufficient to use simple numerical differentiation for these derivatives. The diffusion process should

propagate together with the flow. Our solution to the puzzle is the following.

The convection–diffusion equation

$$\frac{\partial}{\partial t}u + v\frac{\partial}{\partial z}u - \frac{\partial}{\partial z}\lambda\frac{\partial}{\partial z}u = f(u) \tag{30}$$

can be written as two equations:

$$\frac{\partial}{\partial t}u + \frac{\partial}{\partial z}(vu + j) = f(u), \tag{31}$$

$$\lambda\frac{\partial}{\partial z}u = -j. \tag{32}$$

Any numerical method explicit in time would result in an expression which can be put into the source term P, but here the latter equation has been approximated by a partial differential equation of first order,

$$\varepsilon\left(\frac{\partial}{\partial t}j + v\frac{\partial}{\partial z}j\right) + \lambda\frac{\partial}{\partial z}u = -j, \tag{33}$$

where ε is a chosen small parameter $\sim \Delta t$.

A hyperbolic equation system has been created, which has characteristics

$$v_c = v \pm (\lambda/\varepsilon)^{1/2}. \tag{34}$$

To study errors of the method, j can be represented according to Eq. (33) in the form

$$j = -\lambda\frac{1}{\varepsilon}\int_\tau e^{-\tau/\varepsilon}u_z\, d\tau, \tag{35}$$

where the convolution integral is taken in the v-velocity Lagrangian co-ordinate system. If then the derivative u_z is not changed by a great amount during the time interval of the order of ε, the approximation has good accuracy. One can observe that the requirement is not more restrictive than used in general for parabolic equations. The approximate hyperbolic equations technique (AHET) causes the distribution u and its diffusion to propagate together also in the numerical sense.

The equations obtained are of the form in Eq. (1) and can be solved similarly. Hence no separate diffusion model is necessarily needed in the code.

There are also physical reasons for the form in Eq. (33) [2], but here ε has to be chosen purely on a numerical basis. If ε is too large, the diffusion current j does not follow the original definition accurately enough. If ε is too small, the code is not capable of handling the P-term. We suggest choosing $\varepsilon = \Delta t/2$. However, one must be careful not to allow the value of ε to be unreasonably small. The size of the time-step is, of course, dependent on the time scale of the problem.

4. NUMERICAL RESULTS

The numerical experiments calculated by PLIM and presented in this paper are gathered together into Table I. PLIM itself is capable of treating frontal phenomena accurately, but the linear approximation with constant Jacobian matrices in Eqs. (3)–(4) is not necessarily valid in all types of fronts. If the Jacobian matrices do not differ appreciably from each other on both sides of the front, one can expect accurate results.

4.1. *Horizontal Stratified Flow*

In the first two examples the equations are the same as those used for testing the TRAC code [3]. Neglecting friction terms, assuming the interfacial pressure to be constant, and only considering the hydrostatic pressure, momentum and continuity equations can be written in the form

$$\frac{\partial}{\partial t}v + \frac{\partial}{\partial z}\left(\frac{1}{2}v^2 + gh\right) = 0 \tag{36}$$

$$\frac{\partial}{\partial t}A + \frac{\partial}{\partial z}Av = 0, \tag{37}$$

where h = liquid level, A = cross-sectional area of liquid, and v = liquid velocity.

With the notations used in Eq. (1)

$$\begin{aligned}\mathbf{U} &= (v, A)^{\mathrm{T}}\\ \mathbf{F} &= (\tfrac{1}{2}v^2 + gh, Av)^{\mathrm{T}}\\ \mathbf{P} &= (0, 0)^{\mathrm{T}}.\end{aligned} \tag{38}$$

The unknowns are v and h; $A = A(h)$.

TABLE I

Example	Problem definition	Ref.	Figs.
1	Dam break into a stratified water layer	[3]	4–7
2	Dam break into dry channel	[3]	8
3	Sod problem	[4, 5]	9–10
4	Lax Problem	[4, 5]	11
5	Reaction-diffusion	[6]	12
6	Convection-diffusion	[7, 8]	13–14
7	Burgers equation symmetric wave	[9]	15
8	Burgers equation: symmetric wave	[6]	16

EXAMPLE 1. A dam break into a stratified water layer has been solved [3]. There is a 10 m long channel, 1 m in diameter. At time $t<0$ the liquid level (liquid fraction = 0.55) in the left-hand side of the channel is higher than in the right-hand side (liquid fraction = 0.45). At time $t=0$ the dam is removed and the motion of the liquid profile is calculated on both sides of the dam. Both ends of the channel are closed.

In Figs. 4–6 are the results of this problem. The solid line is an analytical solution [3]. A discretization mesh $\Delta t = 0.01$ and $\Delta z = 0.125$ was used in Figs. 4–5, $\Delta t = 0.4$ and $\Delta z = 0.5$ in Fig. 6. The results calculated with PLIM are very good. Even when fairly coarse discretization is used, both the depression wave moving to the left and the bore moving to the right can be described very accurately. TRAC results from [3], where the used maximum timestep $\Delta t = 0.01$ for both space discretizations, make clear how numerical dispersion may affect the solution. Especially interesting is Fig. 6, where PLIM results are obtained with five time-steps, while TRAC has used at least 200 time-steps. In Fig. 7 the formation of the liquid profile is shown.

EXAMPLE 2. Another dam break problem, a dam break into a dry channel, has also been calculated. The difference between this and the first problem is that it is no longer a question of a small perturbation. Here we have a 30 m long channel, 1 m in diameter, where on the right-hand side there is a 10 m long reservoir, where 40% of a cross-sectional area is occupied by liquid. The left-hand side of the channel is open. At time $t = 0$s the dam is removed and the behaviour of the water level in the reservoir is calculated.

In Fig. 8 the water profile is at time 5.6 s. The solid line is an analytical solution [3]. The time when the depression wave should reach the right-hand side of the reservoir is 5.66 s. This is predicted by PLIM quite accurately. The slight error near the break is caused by characteristic velocities, which change their sign there.

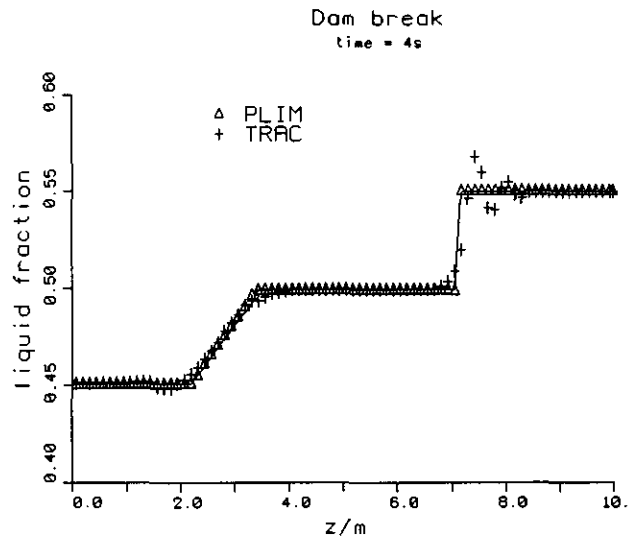

FIG. 5. Liquid fraction profile at time $t = 4$s. The reflected refraction wave and bore moving towards the dam-break. The solid line is an analytical solution. TRAC results are from [3].

4.2. *Gas dynamics*

We have also applied the method for the Euler equations of gas dynamics. Two different Riemann problems known as

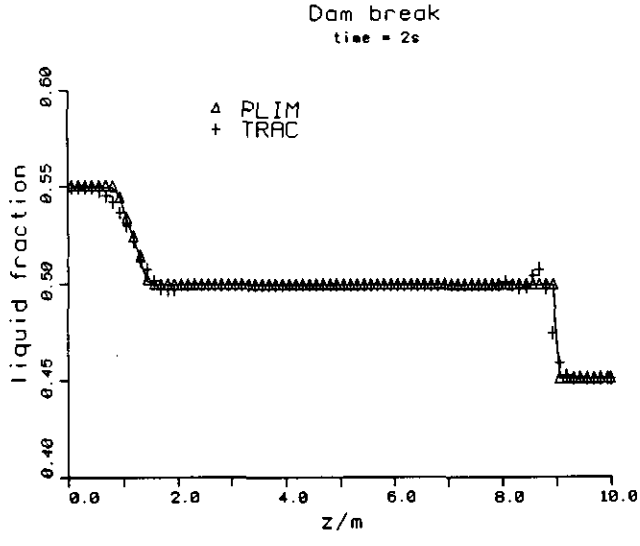

FIG. 4. Liquid fraction profile at time $t = 2$s. The depression wave and bore travelling away from the dam-break. The solid line is an analytical solution. TRAC results are from [3].

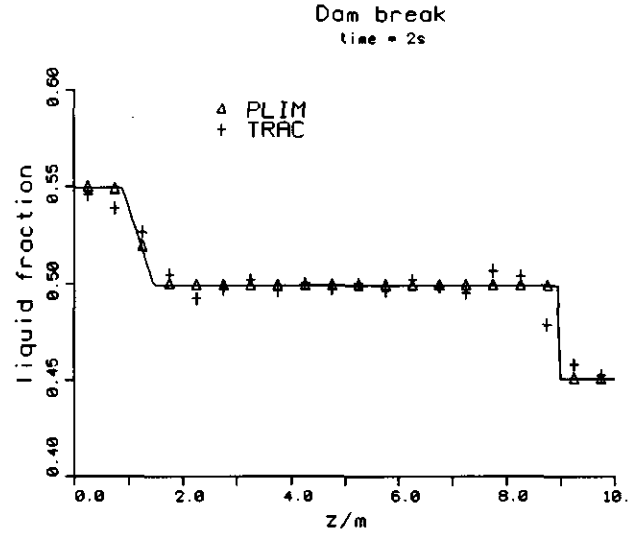

FIG. 6. Liquid fraction profile at time $t = 2$s computed with coarse discretization. The solid line is an analytical solution. TRAC results are from [3].

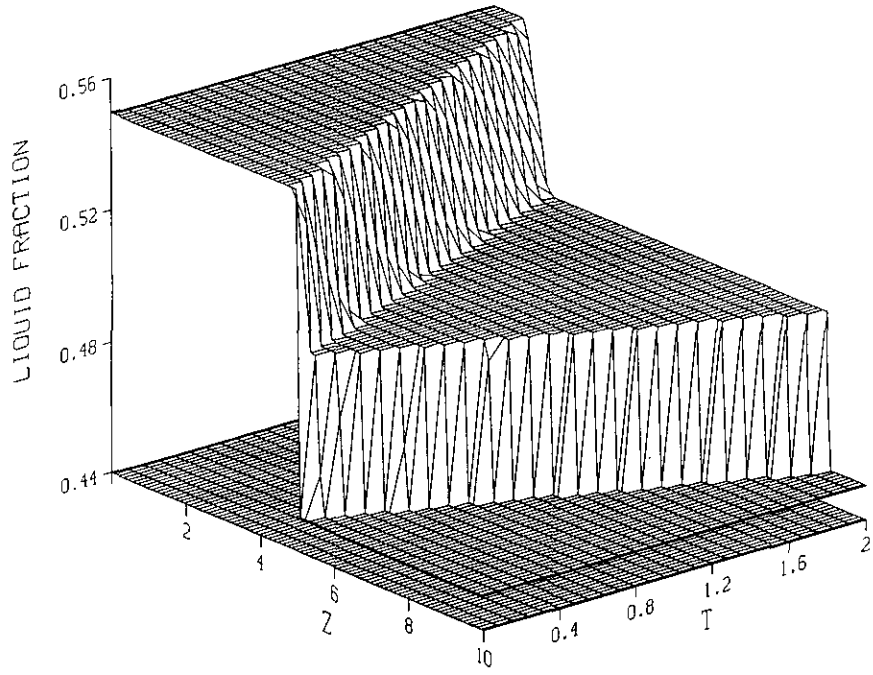

FIG. 7. The formation of the liquid fraction profile in Example 1.

the Sod problem and the Lax problem are solved. The equations used are as in [4, 5]

$$U_t + F(U)_z = 0 \tag{39}$$

$$U = (\rho, m, E)^{\mathrm{T}} \tag{40}$$

$$F(U) = vU + (0, p, vp)^{\mathrm{T}} \tag{41}$$

$$p = (\gamma - 1)(E - \tfrac{1}{2}\rho v^2), \tag{42}$$

where ρ, v, p, E are the density, velocity, pressure, and total energy, respectively; $m = \rho v$ and γ is the ratio of the specific heats, chosen to be 1.4 in the calculations.

In the following Riemann problems, frontal phenomena are formed and hence they are excellent tests for checking the numerical errors.

EXAMPLE 3. In the Sod problem the initial conditions are

$$\begin{aligned}(\rho_L, v_L, p_L) &= (1, 0, 1),\\ (\rho_R, v_R, p_R) &= (0.125, 0, 0.10).\end{aligned} \tag{43}$$

The space discretization used is $\Delta z = 0.1$ as in [4], except in

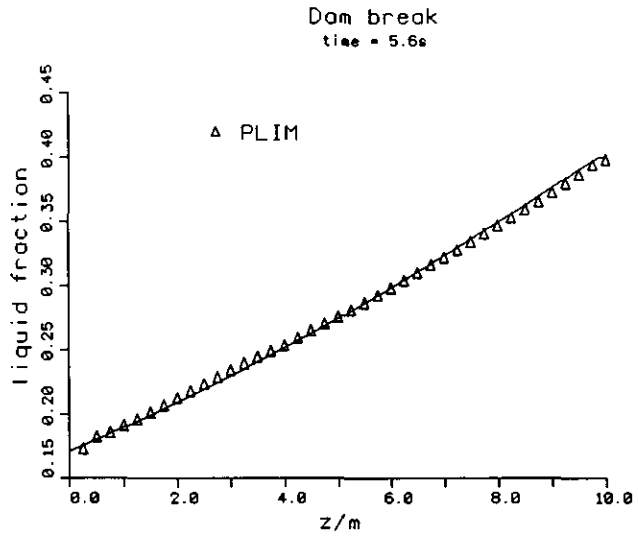

FIG. 8. Liquid fraction profile at time $t = 5.6$s (Example 2). The solid line is an analytical solution.

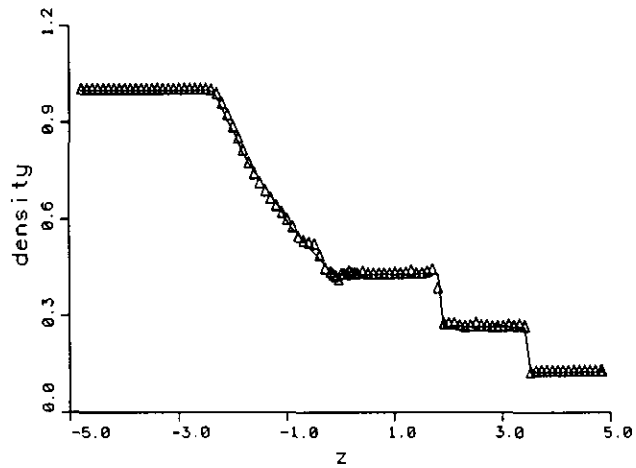

FIG. 9. Sod problem, density distribution at time $t = 2$. Used time-steps are $\Delta t = 0.04$ (solid line), $\Delta t = 0.1$ (plots).

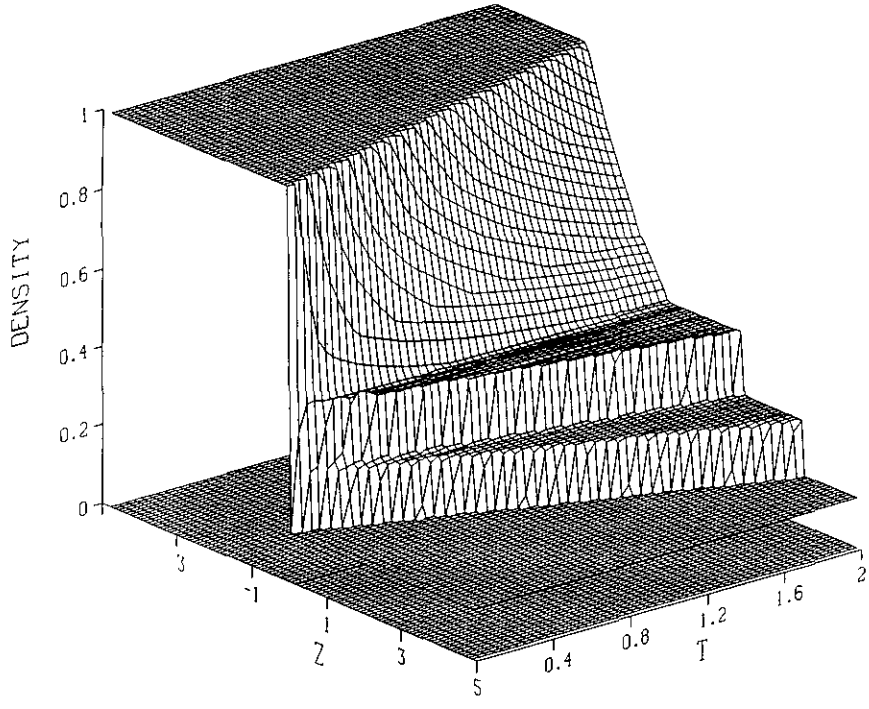

FIG. 10. The formation of the density distribution in the Sod problem.

the middle zone 10 cells have $\Delta z = 0.05$. In Fig. 9 the density distributions at time $t = 2$ are calculated. The time-steps used are $\Delta t = 0.04$ (solid line) and $\Delta t = 0.1$ (plots). When comparing the results to the converged reference solutions in [4, 5], one may regard a solution with $\Delta t = 0.04$ as an exact solution and, even in the solution calculated with longer time-steps, the discontinuities are very sharp, although slight numerical errors do exist, particularly in smoother regions. In Fig. 10 the density distribution is a function of time and place.

EXAMPLE 4. In the Lax problem the initial conditions are

$$\begin{aligned}(\rho_L, v_L, p_L) &= (0.445, 0.698, 3.528),\\ (\rho_R, v_R, p_R) &= (0.5, 0, 0.571).\end{aligned} \tag{44}$$

The space discretization is the same as above but the time-step used is $\Delta t = 0.01$. In this case numerical errors are small as well. The heights of the variations in the density in Fig. 11 may be regarded as accurate when compared to the converged reference solutions in [4, 5]. However, there are some minor oscillations in the solution, obviously because of the constant characteristic velocities used in the mesh cell. The results to these Riemann problems are fully competitive with the calculated results of the ENO schemes presented in [4, 5].

4.3. *A Scalar Reaction-Diffusion Problem from Combustion Theory*

EXAMPLE 5. In this problem an equation of the form [6]

$$\begin{aligned} u_t - u_{zz} &= D(1 + a - u)\exp(-\delta/u) && (45)\\ u_z(0, t) &= 0, \qquad t > 0,\\ u(1, t) &= 1, \qquad t > 0,\\ u(z, 0) &= 1, \qquad 0 \leqslant z \leqslant 1, \end{aligned}$$

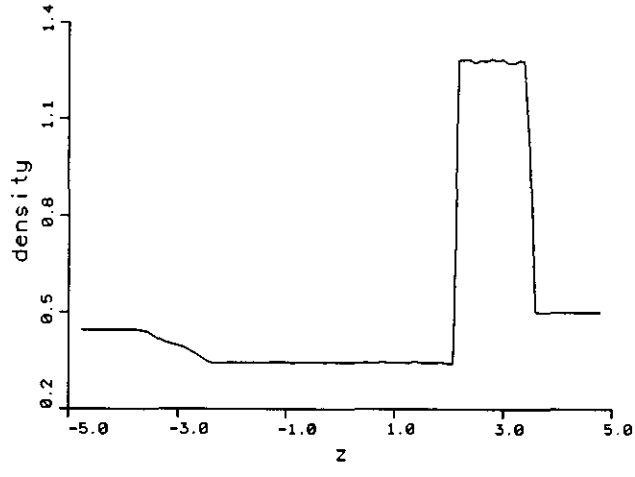

FIG. 11. Lax problem, density distribution at time $t = 1.4$.

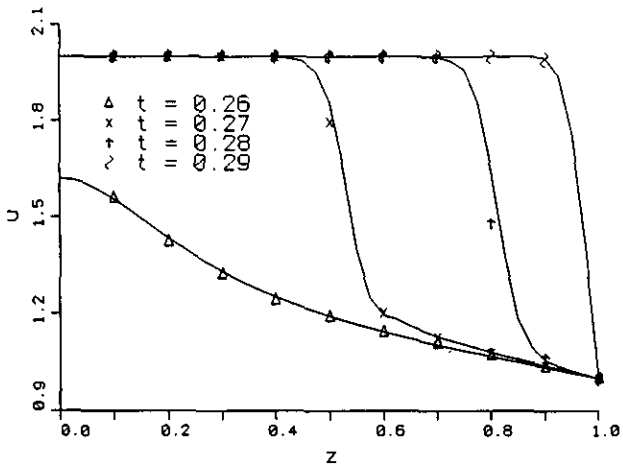

FIG. 12. Temperature distribution in the reaction–diffusion problem at different output times. Plots are from Ref. [6].

where $D = R\exp(\delta)/(a\delta)$ and R, δ, a are constants, was solved using the approximate equtions technique described in Eqs. (31), (33). The solution represents a frontal phenomenon of the temperature of a reactant in a chemical system.

In the beginning of the calculation the temperature gradually increases from unity with a "hot spot" forming at $x = 0$. When ignition occurs the temperature increases rapidly to $1 + a$ and the flame propagates from left to right.

Same parameter values, $a = 1$, $\delta = 20$, $R = 5$, were used as in [6], where this problem has also been used as a test example. It is obvious that the difficulty of the problem is related to the choice of δ. In addition, very short time-steps must be used to describe the propagation of the flame accurately and this may cause problems with approximate equations, because ε in Eq. (33) becomes very small and the handling of the source term is difficult.

In Fig. 12 are the results of the problem. The plots are taken from the figure of Ref. [6], where the output times are $t = 0.26$, 0.27, 0.28, 0.29 and where it is said that the reference solution should be exact, except perhaps in the neighbourhood of $z = 0$ at $t = 0.26$. Results calculated by PLIM are at times $t = 0.259$, etc. This means that the error in time-integration is about 0.001 (10^{-3}). In the beginning, time-steps of size 0.01 were used. Then they were shortened to 0.002 and, when the ignition occurs and the flame propagates rapidly, very short time-steps of size 0.0005 were used. Still the number of time-steps is reasonable, e.g., less than in the calculations in [6]; 41 mesh points were used. Although the reference plots are only estimated from the figure and hence they are not very accurate, it is obvious that the flame propagation can be described accurately with AHET and PLIM.

4.4. *Convection–Diffusion*

EXAMPLE 6. AHET was next applied to solve convection–diffusion problems. With initial conditions

$$u(z, 0) = \sin(z), \qquad z \in [0, 2\pi]$$

and using periodic boundary conditions, Eq. (30) has the exact solution [7]

$$u(z, t) = \sin(z - vt)\exp(-\lambda t).$$

In Fig. 13 the results are at time $t = 1$ and $t = 4$, where $v = 1$ and $\lambda = 0.5$. The discretization used was $\Delta t = 0.1$ and $\Delta z = 0.3927$. Agreement with the numerical solution of the approximate equations and the exact solution of Eq. (30) is good.

Figure 14 shows the results for the test case, where we

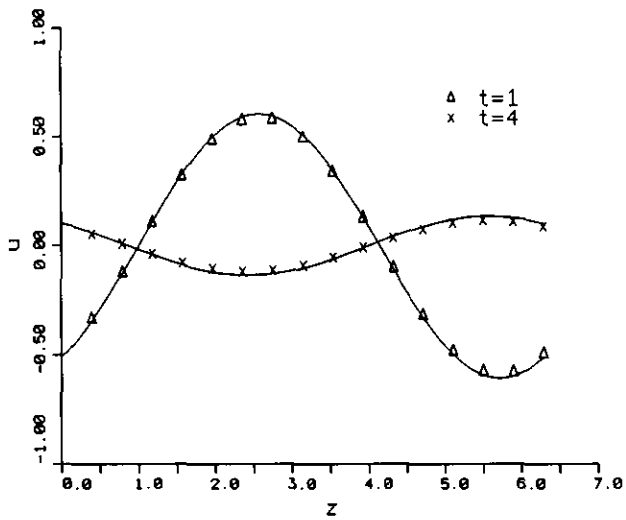

FIG. 13. Convection–diffusion problem. Solutions at time $t = 1$ and $t = 4$. The solid line is an exact solution ($v = 1$, $\lambda = 0.5$).

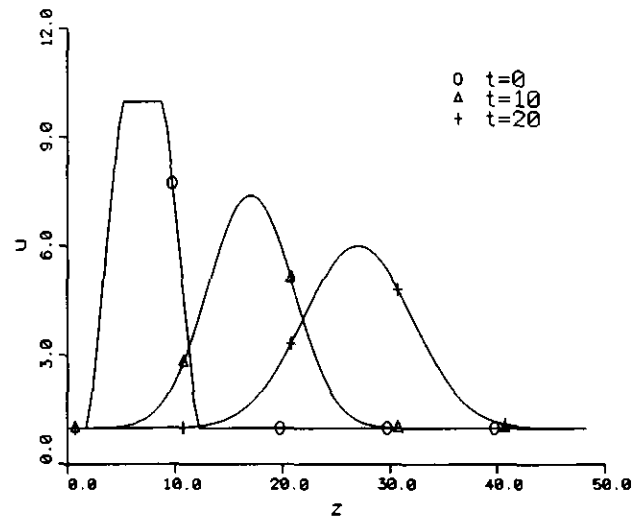

FIG. 14. Convection–diffusion problem. Output times are at $t = 0$, $t = 10$, and $t = 20$ ($v = 1$, $\lambda = 0.5$).

have solved the convection and diffusion of an originally sharp-edged pulse, using $v = 1$ and $\lambda = 0.5$. It is a very good test for the approximate equations technique. We can see that the symmetry of the pulse is conserved. Comparison with the results calculated with the parabolic equation library code of NAG [8] shows that the shape of the pulse is fully correct.

4.5. *Burgers Equation*

Now AHET is applied to a more difficult case, where a non-linear convection term is included. A familiar Burgers equation is of the form

$$\frac{\partial}{\partial t} u + \frac{\partial}{\partial z} \frac{1}{2} u^2 - \frac{\partial}{\partial z} \lambda \frac{\partial}{\partial z} u = 0.$$

EXAMPLE 7. In this test case the following homogeneous Dirichlet boundary conditions were used

$$u(-1, t) = u(1, t) = 0,$$

and the initial state,

$$u(z, 0) = -\sin(\pi z), \qquad -1 \leqslant z \leqslant 1.$$

The solution to this problem develops a very steep gradient in the centre of the domain. After the slope reaches the maximum, it decreases because the initial energy is dissipated away.

As in [9], the viscosity parameter $\lambda = 0.01/\pi$ is chosen. This parameter determines the maximum slope. In Fig. 15 the calculated results are at $t = 0.1$, 0.2, 0.3, 0.4, 0.5. The maximum slope should be reached at time $t = 0.5$ and this is also predicted by PLIM. Comparison with the results of the reference solution in [9] affirms that the Burgers equation

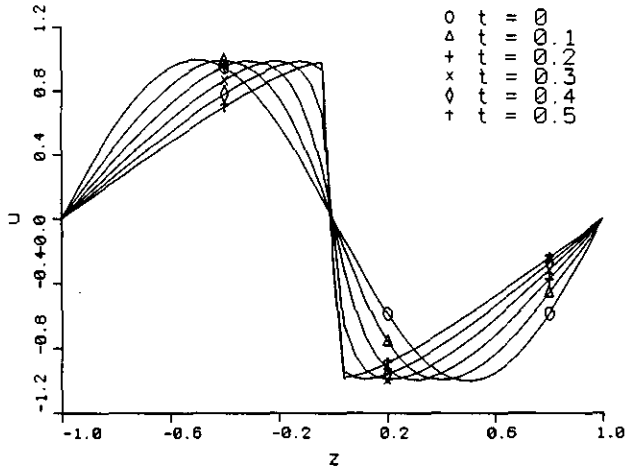

FIG. 15. Burgers equation. PLIM results to symmetric sine wave problem. The maximum slope is reached at $t = 0.5$.

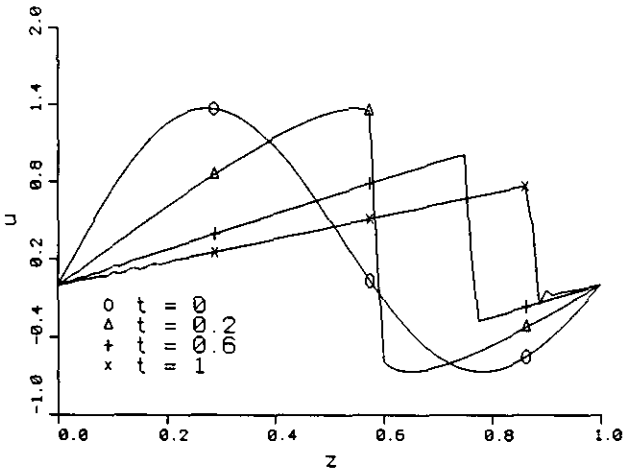

FIG. 16. PLIM solution to Burgers equation with moving shock.

can be solved accurately with the approximation used in this kind of problem. The discretization used was $\Delta t = 0.02$, $\Delta z = 0.04$.

EXAMPLE 8. The same Dirichlet boundary conditions were used as in Example 7, but the initial state was

$$u(z, 0) = \sin(2\pi z) + 0.5 \sin(\pi z), \qquad 0 \leqslant z \leqslant 1.$$

The solution is a wave that first develops a very steep gradient and subsequently moves towards $z = 1$. The viscosity parameter $\lambda = 10^{-4}$; 81 mesh points were used.

Figure 16 shows the results. There are some oscillations near $z = 0$ and near $z = 1$ when $t = 1$. This is caused by characteristic velocities which change their signs in the neighbouring mesh cells. When the results are compared to the reference solution in [6], one can see that there is a slight error in the wave speed from $t = 0.2$ to $t = 0.6$. This may be considered approvable, since the problem is non-linear and because in this problem the value of the viscosity parameter λ is very small and, hence, a very steep gradient is formed and a more accurate solution would require more mesh points to be used in the neighbourhood of the gradient. However, because of the moving wave, an unreasonable dense discretization mesh should be used.

5. DISCUSSION

The generalization of PLIM to two or three dimensions is not straightforward, since the proper multidimensional piecewise linear interpolation shows it to be of enormous complexity. In general the two- or three-dimensional algorithms are obtained by applying a one-dimensional scheme to all the Cartesian directions. The corresponding application of PLIM alone or of PLIM, together with some other scheme, is fully feasible. The domain of the problem is divided into channels. The one-dimensional equations of the

form of Eq. (1) are obtained by integrating over the transverse direction and by removing the transverse fluxes into the source term. Of course, the shape-preserving property of PLIM is then partly deteriorated.

6. CONCLUSION

The applicability and accuracy of a new method PLIM for solving hyperbolic partial differential equation systems has been shown in several frontal phenomena cases. Various difficult flow problems (see Table I), such as the strongly convective problem, the convection–diffusion problem, and the reaction–diffusion problem, have been solved using PLIM, showing the excellent accuracy and the generality of the method. In addition, the approximate hyperbolic equations technique (AHET) produces the corresponding accuracy for parabolic differential equations and derivative terms of second order.

REFERENCES

1. M. Rajamäki and M. Saarinen, in *Proceedings, Int. Topical Meeting Advances in Mathematics, Computations and Reactor Physics, Pittsburgh, PA*, Am. Nucl. Soc., La Grange Park, IL, 1991.
2. K. K. Tamma and J. F. D'Costa, *Numer. Heat Transf. B* **19**, 49 (1991).
3. P. S. Black, D. C. Leslie, and G. F. Hewitt, *Nucl. Eng. Des.* **108**, 121 (1988).
4. H. Yang, *J. Comput. Phys.* **89**, 125 (1990).
5. D.-K. Mao, *J. Comput. Phys.* **92**, 422 (1991).
6. R. M. Furzeland, J. G. Verwer, and P. A. Zegeling, *J. Comput. Phys.* **89**, 349 (1990).
7. G. R. Richter, *Math. Comput.* **54**, 81 (1990).
8. T. Virkkunen, M. Sc. thesis, 1986 (unpublished).
9. M. G. Macaraeg and C. L. Streett, *Int. J. Numer. Methods Fluids* **8**, 1121 (1988).
10. K. W. Morton and P. K. Sweby, *J. Comput. Phys.* **73**, 203 (1987).
11. P. J. Rasch and D. L. Williamson, *SIAM J. Sci. Stat. Comput.* **11**, 656 (1990).
12. A. Staniforth and J. Cote, *Mon. Weather Rev.* **119**, 2206 (1991).